JOINT EUROPEAN TORUS JET

JET–P(93)27

S.V. Neudatchin, D.G. Muir

The Study of Electron Heat Transport in JET Analysing the Decay of Temperature Perturbations induced by Sawteeth

The Study of Electron Heat Transport in JET Analysing the Decay of Temperature Perturbations induced by Sawteeth

S.V. Neudatchin[1], D.G. Muir

JET-Joint Undertaking, Culham Science Centre, OX14 3DB, Abingdon, UK

[1]*Permanent address: I. V. Kurchatov Institute of Atomic Energy, Moscow, Russia.*

Preprint of a paper to be submitted for publication in
Nuclear Fusion
April l993

CONTENTS

Page

ABSTRACT 1

1. INTRODUCTION 1

2. THE MODELLING OF THE HEAT PULSE PROPAGATION 5

2.1 A Description of the Method 5

2.2 The Influence of Heat Sources 8

2.3 The Sensitivity of χ_e^{HP} Values to the Various Parameters 9

2.4 Examples of HPP Analysis and an Interpretation of χ_e^{HP} 11

3. RESULTS FOR 1.5MA AND 3MA DATA 13

3.1 Pulses with ICRH 13

3.2 Pulses with NBI 13

3.3 The Relaxation of χ_e After a Sawtooth Crash 15

4. RESULTS FOR LOW-q-DISCHARGES 16

5. DISCUSSION AND CONCLUSIONS 17

ABSTRACT

A new analysis technique has been developed for the study of the decay rate of sawteeth perturbed T_e profiles to investigate electron transport in the spatial zone between the inversion and mixing radii. The data presented are from JET L and H mode plasmas with currents ranging from 1.5MA to 6MA and with additional heating ranging from 2 to 22MW. Low values of the dynamic electron heat diffusivity χ_e^{HP} were obtained for very good confinement H modes (VH modes) with high values of T_e and ∇T_e. No simple dependence of electron conductivity on T_e or ∇T_e can produce the χ_e^{HP} values obtained in all regimes L, H and VH. However we have found in general that the variations of χ_e^{HP} due to parameter changes were consistent with those observed for the heat diffusivity obtained from power balance calculations.

1. INTRODUCTION

A major problem in understanding the nature of local heat transport in tokamak plasmas is the lack of accurate direct measurements of the local heat fluxes. Typically these fluxes are inferred from detailed power balance calculations. However, these cannot easily separate electron and ion heat fluxes from the total flux, especially in some of the high performance regimes, and the effective heat conductivity, χ_{eff}, obtained from the total heat flux, may not behave similarly to either the ion or the electron conductivity.

The study of electron heat pulse propagation (HPP) has been widely used to obtain information about anomalous electron heat transport in Tokamak plasmas. This report describes a new numerical technique for the analysis of the decay rate of sawteeth perturbed Te profiles in the spatial zone between the inversion and the mixing radii and demonstrates the technique through its application to JET data. This analysis is neither the study of pure outward nor inward HPP but in some sense spread of the initial perturbation in both directions simulataneously. However, this decay can be called heat pulse propagation also.

Many analytical and numerical methods for HPP studies have been developed, in particular, for ECRH induced [1-4] and sawteeth induced heat waves [4-8]. Analytical methods [5, 6] for studying sawteeth induced HPP, assume the electron temperature profile $T_e(r, t)$ evolves in time after the sawteeth crash at radial positions $r \geq r_{inv}$, where r_{inv} is the sawteeth inversion radius, via diffusive

processes with an electron thermal conductivity, χ_e which is constant in time. Similarly, numerical methods [4, 7] also assume a constant χ_e but for $r \geq r_{mix}$, where r_{mix} is the mixing radius defined as the outermost radius where T_e increases after the crash.

The local electron heat conductivity, χ_e, depends on an unknown set of local plasma parameters, e.g. T_e, n_e, and ∇T_e. Local plasma properties are altered by the passing heat wave and so change the value of χ_e. A χ_e dependence on ∇T_e, however, does not affect the diffusive picture of HPP since we can write [2, 3, 6, 18] $\chi_e^{HP} = \chi_e^{PB} + \left(\partial \chi_e^{PB} / \partial \nabla T_e\right) \nabla T_e$; where χ_e^{PB} is the electron conductivity obtained from power balance calculations; $\chi_e^{HP} = \tilde{\Gamma}_e / \left(n_e \nabla \tilde{T}_e\right)$ is the dynamic electron thermal diffusivity, and where $\tilde{\Gamma}_e$ is the electron thermal flux perturbation and $\nabla \tilde{T}_e$ is the electron temperature gradient perturbation. Usually $\chi_e^{HP} > \chi_e^{PB}$ for sawteeth induced and for ECRH induced heat waves [1-8]. This difference can be explained by either a dependence of χ_e on ∇T_e [2, 3, 6, 8, 18, 19], or by the presence of a large convective inward heat flux [2, 8, 18].

The study of the outward propagation of heat waves does not usually allow us to observe the χ_e dependence on ∇T_e or to validate easily simple heat pinch models [18, 2], as was demonstrated in [2] with full transport code calculations. A study of the inward propagation of a flat heat wave (with the temperature gradient close to zero) is needed to separate both conductive and convective heat fluxes, as shown in reference [23] where the anomalous particle convective flux is determined by modelling the inward density wave induced by gas puffing.

Slow inward heat wave propagation has been observed during off-axis ECRH on T-10 [24] and during off-axis ICRH on JET [21]. Slow HPP, with $\chi_e^{HP} \lesssim \chi_e^{PB}$, has also been observed on T-10 [11] when on-axis ECRH was imposed on a broad electron temperature profile created previously by off-axis ECRH. These experiments demonstrated the absence of significant inward convective electron heat fluxes during good electron confinement regimes. However, the experimental data could be described by a complicated heat pinch model [20] in which the inward convective fluxes disappear with large deviations of the T_e profile from the "canonical" one.

Given that anomalous electron transport is governed by mechanisms dependent on local parameters, we can expect that χ_e^{HP} obtained from various sources of

perturbation must be similar in value for plasmas with similar parameters, ∇T_e, T_e etc. This assertion would seem to be correct. Values of χ_e^{HP} obtained from on-axis ECRH induced and sawteeth induced HPP on T-10 [3, 11], and χ_e^{HP} obtained from pellet and sawteeth induced HPP on JET [17] are in reasonable agreement. In addition, the electron temperature perturbation decay at $r_{inv} < r < r_{mix}$ in a calculation made with a full transport code [3], was consistent with the $\chi_e^{PB}(\nabla T_e)$ model used. These results imply that, in these regimes, sawteeth induced HPP is a manifestation of transport only and not of any other process. However, comparisons of χ_e^{HP} values obtained from various sources of perturbation have not yet been done systematically.

The opposite point of view whereby the turbulence associated with a sawteeth crash affects the HPP in an unpredictable manner was suggested in [10]. It was shown in reference [10], from measurements made in the TFTR tokamak of the electron temperature profile evolution during a sawteeth crash, that significant heat was deposited beyond the mixing radius r_{mix} within 200 μsec following the crash. Only one example was given. In their opinion, χ_e immediately after the crash was strongly enhanced. A fast relaxation of χ_e to its original level then occurred. It was declared that the transport results obtained previously on the TFTR and JET were distorted to an unknown degree by this effect. The example from [10] was reanalysed in reference [9]. The authors of [9] concluded that the variation in χ_e with time exists and that this χ_e enhancement is smaller the greater the distance from the inversion radius. In their opinion, HPP can be studied with standard methods at $r > r_{mix}$.

Some disagreement between χ_e^{HP} values obtained by different methods was seen in one regime on T-10. The χ_e^{HP} values estimated from an analysis of the sawteeth induced $\tilde{T}_e$ decay rate (within 1ms after a crash) at $r \approx r_{mix}$ with 1MW of on-axis ECRH in low density plasmas were at least two times greater than χ_e^{HP} obtained from instability induced heat wave propagation in the same region [15].

Given the various points of view discussed above, the results obtained in some regimes by different groups have been contradictory. Additional study is needed to understand when and in what plasma region sawteeth induced HPP can be affected by a χ_e relaxation in time.

It is often very difficult to determine the location of the space-time boundary between short timescale enhanced transport effects and the traditional outward heat wave. To avoid these problems, consider that outermost normalised radius where the electron temperature is seen to be increasing within 1ms (for JET timescales) after the beginning of the sawteeth crash. At the end of this time the relaxation of χ_e has probably ended and the temperature gradients are relatively smooth. This radius will be denoted r_{mix1} to avoid confusion with other definitions of the mixing radius used. For some 6MA and 7MA JET pulses, $r_{mix1} \approx 0.85$. For many pulses with additional heating and irregular or monster sawteeth, HPP at $r > r_{mix1}$ could not be studied due to the low amplitude of perturbations. The method described in this report enables, for the first time, HPP analysis in the region $r_{inv} < r < r_{mix1}$.

To investigate electron transport in the zone between the inversion radii r_{inv} and r_{mix1} and to estimate the influence of enhanced transport, a method [4] was developed for the analysis of the decay rate of the initial sawteeth induced T_e perturbation. For this zone, we can separate in time the crash event from the transport under study by beginning the analysis of HPP a few milliseconds after the crash, taking the perturbation profile directly from experimental data. For $r > r_{mix1}$, the perturbation profile is uncertain. Varying the time delay allows us to either exclude or to study the possible influence of the relaxation of χ_e on χ_e^{HP}. The high amplitude of the perturbation in the region $r_{inv} < r < r_{mix1}$ also allows us to study HPP from each crash individually.

The paper is organised as follows: In section 2 the method is presented. Questions concerning the sensitivity of the results obtained to the damping terms and to the experimental data errors are discussed. The essential points of the method are demonstrated with results from a study of high density 3MA plasmas with central and mixed (on and off axis) ICRH. Problems arising from the possible influence of χ_e (∇T_e, T_e) dependence on the χ_e^{HP} values obtained are also discussed. A comparison of χ_e^{HP} data for ICRH heated 3MA and 1.5MA plasmas is presented in section 3. Examples of HPP in NBI heated L and H mode discharges are also presented. Similarly, results for 6MA pulses are discussed in section 4. The report is summarised in section 5.

2. THE MODELLING OF THE HEAT PULSE PROPAGATION

2.1 A Description of the Method

The electron temperature profile before and after a sawteeth crash is illustrated in Fig. 1 with data from the JET pulse 27578. Energy from the core of the plasma is transferred to the plasma region $r_{inv} \lesssim r \lesssim r_{mix1}$ and is seen as a perturbation of the temperature profile. Later this perturbation diminishes with time due to both a decrease in the heat outflux from the core of plasma and the outward propagation of the electron temperature wave into the region $r > r_{mix1}$. The profile eventually returns to a quasi-steady state form. The time evolution of the electron temperature profile, demonstrating several sawteeth events at several plasma positions, is shown in Fig. 2. The $T_e(r, t)$ decay during one of the many sawteeth events seen is shown in greater detail in Fig. 3. It is the study of this decay that forms the basis of the new method presented here.

The electron temperature in JET is measured using a variety of diagnostic systems. Of particular use to the study of HPP is data from the ECE grating polychromator. This diagnostic provides temperatures at several plasma positions in the horizontal mid-plane with high time resolution [25]. Referring to Fig. 2, there are several spatial positions inside the region $r_{inv} \leq r \leq r_{mix1}$. The radial position of the measurement point closest to and outside of the inversion radius is denoted r_1, and the radial position of the measurement point closest to r_{mix1} is denoted r_3. The temperature data at r_1 and r_3, together with all data at measurement positions $r_1 < r < r_3$, denoted r_{2i}, where i is an integer number, are used to solve the transport equation for χ_e^{HP}.

It is seen from Figs. 2-3 that within one millisecond from the beginning of the crash the electron temperature perturbation has spread well away from r_{inv} but has no clear outer boundary. Moreover, in some low q JET pulses, we have found that the perturbation had spread up to $r \approx 0.85$ within 1 ms after the beginning of the crash (see e.g. Fig. 14). Our experience with JET data has indicated that the traditional concept of a mixing radius could not be easily applied and clarifies why a new definition, r_{mix1}, is used.

The time evolution of the temperature profile is determined by the local electron heat transport and by the local heat sources and sinks. Starting with the equation for conservation of energy we have

$$\frac{3}{2}\frac{\partial n_e T_e}{\partial t} = \nabla(\Gamma_e) + Q_e \qquad (1)$$

where Γ_e is the local electron heat flux $\Gamma_e = -\chi_e n_e \nabla T_e + \frac{5}{2}\Gamma_n T_e$, n_e is the electron density, Q_e is the sum of local heat sources and sinks, i.e. $Q_e = \Sigma_{sources} - \Sigma_{sinks}$, and Γ_n is the electron density flux. Let us write all terms as the sum of a steady state and a perturbed value i.e. $T_e = T_{e_o} + \tilde{T}_e$, $n_e = n_{e_o} + \tilde{n}_e$, $\chi_e = \chi_{e_o} + \tilde{\chi}_e$, etc. For most JET sawteeth crashes the relative value of the density perturbation is significantly less (by an order of magnitude) than the relative electron temperature perturbation, i.e. $|\tilde{n}_e / n_e| << |\tilde{T}_e / T_e|$. Therefore $\tilde{n}_e$ can be ignored. The role of the perturbation to the term $5/2\ \Gamma_n\ T_e$, is less obvious. However, the term $\tilde{T}_e\ \Gamma_n$ is probably insignificant because it has been observed that $D << \chi_e^{HP}$ for JET [17]. To the author's knowledge, no evidence has been found for the influence of the coupled transport term $\tilde{\Gamma}_n$ (variations in density flux caused by $\tilde{T}_e$) on the electron HPP on JET. A more detailed discussion on the problems of electron density transport lies outside the scope of the present work.

Taking into account all the above simplifications, equation (1) becomes

$$\frac{3}{2} n_e \frac{\partial \tilde{T}_e}{\partial t} = \nabla \cdot \left(\tilde{\Gamma}_e\right) + \tilde{Q}_e = -\nabla \cdot \left(n_e \chi_e^{HP} \nabla \tilde{T}_e\right) + \tilde{Q}_e \qquad (2)$$

where $\chi_e^{HP} \equiv -\tilde{\Gamma}_e / \nabla \tilde{T}_e\ n_e$ is the dynamic electron thermal diffusivity, $\tilde{\Gamma}_e$ is the electron thermal flux perturbation and $\tilde{Q}_e$ is the perturbation of the electron heat source.

Equation (2) is solved numerically in the region $r_1 \le r \le r_3$ (see Fig. 3) with the initial conditions provided by experimental measurements $\tilde{T}_{e\ calc}(r,0) = \tilde{T}_{e\ exp}(r,0)$. Furthermore, as boundary conditions, the experimental data at $r = r_1$ and $r = r_3$ are used:

$$\tilde{T}_{e\ calc}(r_1,t) = \tilde{T}_{e\ exp}(r_1,t),\ \tilde{T}_{e\ calc}(r_3,t) = \tilde{T}_{e\ exp}(r_3,t)$$

The initial condition (t = 0) was chosen about $t_o \approx 2$ms after the beginning of the crash. This shift in time was needed to avoid possible short time scale fast transport immediately following the sawteeth crash and to avoid the rapidly changing gradients.

Equation (2) was solved, in cylindrical geometry (JET ellipticity and shift were taken into account by assuming $r(R) = (R - R_o(R))\sqrt{(\lambda^2(R)+1)/2}$ where R is the mid-plane major radius, R_o (R) is flux surface centre and λ is the ellipticity), using an implicit conservative difference scheme. The difference problem was solved with a three point Gauss elimination method. The positions of the ECE channels were obtained by matching the cyclotron frequencies with the total magnetic field profile calculated by the equilibrium solver IDENTC [22].

Consider initially the situation when $\tilde{Q}_e = 0$. The calculated values of $\tilde{T}_e(r_{2i}\ t)$ from the inner ECE channels r_{2i} would then depend only on the unknown value of χ_e^{HP}. One can determine the optimum value χ_e^{HP} automatically from the best fit to the calculated and experimental data from the inner polychromater channels at $r_1 < r_{2i} < r_3$ (see Fig. 3), by minimising the difference $M = \sum_{i=1}^{n} \int_{o}^{t1} \left[\tilde{T}_{calc}\left(\chi_e^{HP}, r_{2i}, t\right) - \tilde{T}_{exp}(r_{2i}, t)\right]^2 dt$.

Fig. 3 shows examples of the solution of equation (2) for three different values of χ_e^{HP}. It is clear that the central solution provided a good fit to the data. At least 20 calculations with various χ_e^{HP} were done to find the minimum of M. The dependence of M on the normalised χ_e^{HP} value for the crash in Fig. 3 is shown in Fig. 4.

In practice, the problem is more complicated when χ^{HP} has a radial dependence. Values of χ_e^{HP} were obtained initially for χ_e^{HP} = constant (20 calculations), for $\chi_e^{HP} \sim \sqrt{r}$ (again 20 calculations) then again for $\chi_e^{HP} \sim r$ etc. The minimum values of M, obtained for each class of radial dependence, were then compared to determine the most appropriate radial

dependence. Curiously, the values of χ_e^{HP} at $r = \frac{1}{2}(r_1 + r_3)$ were almost the same for various values of γ, i.e. all curves $\chi_e^{HP} \sim r^\gamma$ for $\gamma = 0, 0.5, 1$ usually crossed in the middle of the region studied. For most pulses , the best fit was obtained with a weak radial dependence: $\chi_e^{HP} \sim \sqrt{r}$.

The high amplitude of the perturbation in the region $r_{inv} \lesssim r \lesssim r_{mix1}$ allows us to study each crash separately and to improve the accuracy of our χ_e^{HP} measurements statistically even when a limited number of crashes, with various amplitudes, exist. Let us name this method the " mixture" method because it uses both initial and boundary conditions.

It is clearly seen from figures 1-3 that we are studying the decay of the perturbation in a space region where the values of $\nabla \tilde{T}_e$ have opposite signs on left and right boundaries during the time period of analysis. We are not studying either pure outward or pure inward HPP, but the spread of the initial perturbation in both directions together. In this sense, the decay can be called heat pulse propagation.

2.2 The Influence of Heat Sources

Let us now discuss the sensitivity of this mixture method to the heat source perturbations. The electron heat source perturbation $\tilde{Q}_e$ is composed from at least three terms:

$$\tilde{Q}_e = \tilde{Q}_{joule} + \tilde{Q}_{ei} + \tilde{Q}_{e_{add}}$$

The perturbation of the joule heating term $\tilde{Q}_{e_{joule}} \sim - \tilde{T}_e$ is not significant for all the pulses studied so far. However, the equipartition term, $\tilde{Q}_{e_i} \sim \tilde{T}_e / \tau_{ei}$, can be significant and must be taken into account. The role of this term is strongly dependent on the plasma conditions and the sawteeth location. Moreover, for some pulses the possible perturbation of the ion temperature, T_i, could have been comparable to that of T_e. The magnitude of $\tilde{Q}_{e_i}$ has been estimated separately for each pulse analysed and for most pulses was not important. The third term

$\tilde{Q}_{e_{add}}$ represents the variation in additional heating and has not been taken into account. One can see from Fig. 2 the negative value of $\tilde{T}_e$ between crashes. This effect was clearly seen in various plasma regimes. It is possible that the $\tilde{Q}_{e_{add}}$ term is responsible for this over-relaxation in $\tilde{T}_e$. One possible reason is that this cooling may have been due to a distortion in the electron/ion distribution function during the crash. The influence of this effect for each pulse (or crash) can be estimated directly from the experimental data by assuming $\tilde{Q}_{e_{add}}(r) = \frac{3}{2} n_e \frac{\partial \tilde{T}_{e_{exp}}(r)}{\partial t}$ when $\tilde{T}_{e_{exp}}(r) = 0$.

Outside r_{mix1} the influence of $\tilde{Q}_{e_{add}}$ could have been significant due to the low amplitude of $\tilde{T}_e$. In the results presented below, the influence of $\tilde{Q}_{ei}$ and $\tilde{Q}_{e_{add}}$ typically gave rise to insignificant corrections to the calculated values of χ_e^{HP}. A typical correction was approximately 10% (within the zone $r_{inv} \leq r \leq r_{mix1}$).

2.3 The Sensitivity of χ_e^{HP} Values to the Various Parameters

Let us introduce an index to the "quality" of the heat waves. The index is the "relative sharpness" of the heat wave and is defined:

$$S = << / \frac{\nabla \tilde{T}_e}{\tilde{T}_e} / \frac{\nabla T_{eo}}{T_{eo}} / >> \qquad (3)$$

averaged in space. This is the experimental characterization of the sensitivity of conduction term (χ_e^{HP}) to "convective-like" terms (source perturbation, $\chi_e(t)$ and $\chi_e(T_e)$ dependence, $\Gamma_n \tilde{T}_e$ etc.) For example, if S = 3 and $\chi_e^{HP} = 2\chi_e^{PB}$, this would mean that χ_e^{HP} is $S\chi_e^{HP}/\chi_e^{PB} = 6$ times less sensitive to variations in the source terms than is χ_e^{PB}. The value of S particularly depends on the locations of the polychromater channels. The channel at $r = r_1$, must be located just outside r_{inv}. The value of S decreases in time due to a spreading of the initial perturbation. This is the

reason why the HPP study is bounded in time. Let us use S averaged over the time interval of the HPP analysis for our measure of quality.

The "mixture" method is not sensitive to the absolute value of $T_e(r)$ or to the radial positions of the region studied. However, errors in $\nabla T_e/T_e$ and in the distance between ECE channels $r_i - r_{i+1}$ can have a direct influence on the value of χ_e^{HP}. The effect of systematic errors in the $\tilde{T}_e$ measurements could be calculated for each crash separately. An example of the sensitivity of the calculation to χ_e^{HP} values is shown in Fig. 3. The form of the square difference between calculated and experimental data $M(\chi_e^{HP})$ curve (see Fig. 4) is also an important characterisation of the sensitivity of χ_e^{HP} values obtained to the errors. The sharp minimum of the $M(\chi_e^{HP})$ curve represents a stable and well known χ_e^{HP} value, and vice versa. The sharpness of the $M(\chi_e^{HP})$ curve is related to the sharpness of $\tilde{T}_e$ (r, t) i.e. to the S value. Stable values of $\nabla \tilde{T}_{e_{exp}}(r,t)$ with opposite signs on the left and right boundaries are also needed for a well defined M minimum. For good pulses with $S \geq 2$, a systematic 10% perturbation of $\tilde{T}_e$ on both boundary channels (or on all the inner channels together) gave approximately the same shift in the value of χ_e^{HP}. For example, a 10% increase in $\tilde{T}_e$ on both boundary channels for pulse 27578 resulted in a 12% increase in χ_e^{HP}. For pulses with a lower value of S, the error in χ_e^{HP} can be larger.

Another possible source of error was the quality of the initial $\tilde{T}_{e_{exp}}$ (r, 0) profile. At least two inner channels were needed to have a satisfactory initial perturbation profile.

The application of the new method with a more realistic geometry would result in a systematic slight reduction of χ_e^{HP}. This would be larger for the outermost region.

An estimation of the total random error in the value of χ_e^{HP} was provided by the natural variance in the χ_e^{HP} values obtained for each individual crash.

The variation of χ_e^{HP} with time was studied by varying the time interval between the beginning of the crash and the start of the HPP study, t_0. The integration time period t_1 was also varied. However, there were limited possibilities in choosing the values of t_0 and t_1 because the time period $(t_0 + t_1)$ was constrained by the decay of the perturbation profile. The maximum value of $(t_0 + t_1)$ varied from 10 to 30ms for various pulses. Results from this study are discussed in section III.

2.4 Examples of HPP Analysis and an Interpretation of χ_e^{HP}

The method was applied to high density plasma regimes with on axis 10MW (pulse 27578) and mixed (on + off) 10MW ICRH heating (pulse 27579) [12]. A comparison of the χ_e^{HP} obtained with χ_{eff} values from power balance calculations are shown in Fig. 5. The errors in χ_e^{HP} shown in figure 5 represents the variance in the calculated data (8 crashes in each pulse). The HPP at $r > r_{mix1}$ could not be studied for pulse 27578 due to the low quality of the T_e measurements, nor for pulse 27579 due to the influence of $\tilde{Q}_{e_{add}}$. Let us now discuss the problem of interpretation of the χ_e^{HP} values obtained.

In the region studied, the initial value of $\nabla\tilde{T}_e$ was significant and the total gradient ∇T_e varied in time and space. It is well known [2, 3, 6] that when the electron heat diffusivity measured by power balance $\chi_e^{PB} = \chi_e(\nabla T_e, T_e)$ the expression for χ_e^{HP} becomes

$$\chi_e^{HP} = \chi_e^{PB} + \frac{\partial \chi_e^{PB}}{\partial \nabla T_e} \nabla T_e + \frac{\partial \chi_e^{PB}}{\partial T_e} \frac{\tilde{T}_e}{\nabla \tilde{T}_e} \nabla T_e \qquad (3)$$

where $\nabla T_e = \nabla T_{eo} + \nabla\tilde{T}_e$ is the total gradient.

A problem for both pulses was that while χ_{eff} was well-defined, χ_e^{PB} was not (due to the uncertainty with the equipartition term). Let us suppose that $\chi_e^{PB} = 0.8\sqrt{r/r_1}\ m^2s^{-1}$ for pulse 27578, and consider the validity of (3) for the mixture method with a dependence of χ_e^{PB} on ∇T_e. If χ_e is dependent on ∇T_e only and we have both χ_e^{HP} (see figure 5) and χ_e^{PB}, then one can obtain the term $\left(\partial \chi_e^{PB} / \partial \nabla T_e\right)\nabla T_e$ from (3):

$$\left\langle \left(\partial \chi_e^{PB} / \partial \nabla T_e \right) \nabla T_e \right\rangle_t = \chi_e^{HP} - \chi_e^{PB} \approx 1.4 \sqrt{r / r_1} \ m^2 s^{-1}.$$

A generalised set of calculations with $\chi_e^{HP} = (0.8+\alpha(\nabla T_{eo}+\nabla \tilde{T}_e)) \sqrt{r / r_1}$ $m^2 s^{-1}$, where α is analogous to $\partial \chi_e^{PB} / \partial \nabla T_e$, was done in order to check the estimation above. Values of α were determined by finding the minimum in the sum of the square differences between calculated and measured temperature data for each crash separately and after averaging a value of $\alpha(r)\ \nabla T_{eo}(r) = 1.16 \pm 0.22 m^2 s^{-1}$ was obtained. The reasonable agreement found between the values obtained above means that the simple relationship (3), averaged in time, is a good representation of χ_e^{HP} even when ∇T_e varies significantly in time and space.

The next step is to examine the $\chi_e(T_e)$ dependence. For $\chi_e^{PB} \sim T_e^{\sigma}$, equation (3) can be rewritten as

$$\chi_e^{HP}(r,t) = \chi_e^{PB} + \sigma \chi_e^{PB} \frac{\tilde{T}_e}{\nabla \tilde{T}_e} \frac{\left\langle \nabla T_{eo} + \nabla \tilde{T}_e \right\rangle}{T_{eo}}; \ \tilde{T}_e / T_{eo} << 1 \qquad (4)$$

which, after averaging in time becomes

$$\chi_e^{HP} \equiv \langle \chi_e^{HP}(r,t) \rangle_t = \chi_e^{PB} \left(1 + \frac{\sigma}{S} + \sigma \frac{\left\langle \tilde{T}_e \right\rangle_t}{T_{eo}} \right) \qquad (5)$$

A value $\sigma \approx 2.5$ for both pulses was obtained from (5) when it was assumed that $\chi_e^{PB} = 0.8\ \chi_{eff}$ for both the mixed heating and the central heating cases. A comparison of heat fluxes in these pulses was done previously in [12]. It was shown that the variation in χ_{eff} could be connected with the variation in ∇T, otherwise χ_{eff} would have to have a strong temperature scaling, e.g. $T^{2.5}$ (it was supposed that $T_e \equiv T_i = T$ in these high density plasmas). These results, together with the results from the present HPP study, suggest a χ_e dependence on ∇T_e or on a mixed $\chi_e = \chi_e\ (T_e, \nabla T_e,)$ dependance, but not on a simple Te dependence only.

3. RESULTS FOR 1.5MA AND 3MA DATA

3.1 Pulses with ICRH

A comparison of χ_e^{HP} values obtained for on-axis ICRH heated 1.5 and 3MA plasmas with $B_z \approx 3T$ together with the power balance χ_{eff} values are shown in Fig. 6. The χ_{eff} valves used were obtained either from TRANSP analysis (see the brief description of TRANSP in [13]) or from CHAIN-2 [26]. It is seen that the variations in χ_e^{HP} are consistent with the changes in χ_{eff} when the plasma current varies from 1.5MA to 3MA [12, 14]. In order to compare χ_e^{HP} in 3MA plasmas with those of 1.5MA plasmas, consider the very simple temperature and radial dependence

$$\chi_e^{HP} = f(r\ T_e(r) / r_{inv})^{3/2} r \qquad (6)$$

where f is a constant. This approximate relationship usually is in reasonable agreement with the weak radial dependence in χ_e^{HP} found for most pulses. A comparison of the f-values obtained for the zone $(r_1 + r_3)/2$ are shown in Fig. 7. Results for low-quality HPP with $S < 2$ are indicated by additional circles. More 1.5MA pulses need to be analysed, but the values of f appears higher in general for 1.5MA plasmas than for 3MA.

3.2 Pulses with NBI

A similar analysis was done for 3MA NBI-heated plasmas in L and H modes with $B_z \approx 3$ T. The χ_e^{HP} results obtained are shown in Fig. 7 as squares. One can see that low χ_e^{HP} values with very low values of f existed in some pulses with NBI. These points are from heat pulse propagation from single sawteeth crashes in hot ion H mode pulses. f can vary through one order of magnitude for various 3MA pulses. This means that the simple $T_e^{3/2}$ dependence (6) does not give a reasonable fit to the whole data set.

Radial dependencies of the form

$$\chi_e^{HP} = \text{const} \cdot r^{\gamma} / r_{inv}^{\delta}\ T_e^{x} \qquad (7)$$

with x = 1 or 1.5 and various γ and δ (γ and δ are connected if we assume χ_e^{HP} has a reasonable radial dependence) were also checked. The results obtained were similar to that shown in Fig. 7. Therefore these simplest relationships (7) cannot represent the χ_e^{HP} values obtained for L, H and hot ion H modes plasmas.

Let us consider the changes in χ_e^{HP} with the transition from L mode to hot ion H mode in more detail. In the two identical pulses, 26290 and 26292, the NBI power was initially 2MW and was increased to about 11MW in the hot ion H mode phase. The values of χ_e^{HP} for the 2MW L mode period and χ_e^{HP} at the end of the hot ion H mode are shown in Fig. 8. Unfortunately we could only obtain the upper limit of χ_e^{HP} for hot ion H mode crashes because the location of r_1 was too close to the inversion radius to provide a suitable boundary condition. However, it was estimated that the real value of χ_e^{HP} was probably 20-30% lower. It is clearly seen from Fig. 8 that χ_e^{HP} does not increase on making the transition from a 2MW NBI L mode to a 11MW hot ion H mode. In fact it decreased for a 13MW H mode in pulse 26801 (curve 3 on Fig. 8). The $T_e(r)$ profiles for these pulses are shown in Fig. 9. The value of T_e (R = 3.6m) increases by an approximate factor 4 from curve 1 to curve 3 in Fig. 9, while χ_e^{HP} decreases. Similar low values of χ_e^{HP} were obtained for the near identical pulse 26792 and for the 15MW hot ion H mode pulse 26764. The correlation between low values of χ_e^{HP} and high confinement is clearly seen. No known simple dependence χ_e (T_e,∇T_e) can produce the χ_e^{HP} values obtained in Fig. 8 together with those in Figs. 5 and 6.

Let us now consider the changes in χ_e^{HP} during various stages of an H mode. The evolution of T_e (r = 0.35, t), $P_{NBI}(t)$ and stored energy W(t) for pulses 26792 and 26801 are shown in figures 10 and 11 respectively. Each pulse had two crashes which occurred during the H mode. In pulse 26792, χ_e^{HP} was at least 1.8 times higher for the second crash than for the first. The observed increase in χ_e^{HP} was well correlated with the decrease in energy confinement. For this second crash, the slow decay of $T_e(r, t)$ began after the reduction of NBI power from 14MW to 7MW. This was taken into account in our calculations. The value of χ_e^{HP} was 1.3 times higher for the second crash (P_{NBI} = 7MW) than for the first in pulse 26801. The HPP at $r > r_{mix1}$ was very slow for this crash. A value $\chi_e^{HP} < 0.7\ m^2s^{-1}$ for $r > r_{mix1}$ was obtained with the one boundary method [4]. Confinement

remained high following this crash. The difference in χ_e^{HP} between the first and second crashes in pulses 26801 and 26792 is evidence for the correlation between χ_e^{HP} and energy confinement during the plasma evolution through the H mode stage.

The relationship between χ_e^{HP} and χ_{eff} for a wide range of pulses is shown in Fig. 12. Pulses with I_p from 1.5 to 5MA, and various heating scenarios ICRH, NBI, ICRH + NBI, with additional power from 2 to 22MW and with ^{4}He, D, H gas fill are presented. It is seen from Fig. 12 that, in general, the variations of χ_e^{HP} due to parameter changes are not incompatible with those observed for χ_{eff}.

For most of the pulses studied the amplitude of the density perturbations was either very small or was not seen in the interferometer signals. However, for some pulses the electron density perturbation was stronger and possibly could have affected HPP in some crashes.

3.3 The Relaxation of χ_e After a Sawtooth Crash

For the results presented above, the time period between the beginning of the crash and the beginning of the HPP study, t_0, was typically about 2 ms (see Fig. 3). The question concerning the sensitivity of the observed χ_e^{HP} to t_0 naturally arises. Increasing t_0 from 2ms to 6ms (with t_1 = 12 and 8ms respectively) gave approximately a 20% decrease in χ_e^{HP} while increasing t_1 from 8 to 16ms (with t_0 = 2ms) gave a 10 - 15% reduction. These reductions were stronger in the hot ion H mode. For example, for pulse 26801, χ_e^{HP} (t_0 = 2ms, t_1 = 8ms) $\approx 2\,\chi_e^{HP}$ (t_0 = 6ms, t_1 = 16ms). Similar results were obtained for pulses 26792 and 26764. Moreover, χ_e^{HP} for pulse 26792 was close to $0.5 m^2 s^{-1}$ after the relaxation of χ_e.

Approximately half of the observed variation in time can be explained by a linear dependence of χ_e on T_e and ∇T_e (but not for the hot ion H mode). This implies that χ_e^{HP} could be constructed from two parts: $\chi_e^{HP}=\chi_{eo}^{HP}(r, t) + \chi_{eadd}^{HP}(t)$, where $\chi_{eadd}^{HP}(t) \approx \alpha\chi_{eo}^{HP}\, e^{-t/\tau}$. (t = 0 corresponds to that time delay t_0). The values of α and τ are correlated and for $\tau \approx$ 5ms, $\alpha \approx 0.7$ (t_0 = 2ms). There is obviously a complicated relationship between $\chi_{eadd}^{HP}(t)$ and the real variation of electron conductivity in time and space: $\chi_e = \chi_e^{PB}(T_e \nabla T_e, ..) + \chi_{eadd}(r, t)$. The observed value of the ratio

$\chi_{e_{add}}(0)/\chi_e^{HP}(0) \approx 0.1 \sim 0.2$ (with $t_0 = 2$ ms) and has a complicated variation in time and space. For the hot ion H mode, χ_{eadd} (0) ~ 0.4 $m^2\ s^{-1}$ (t_0 = 2ms).

The picture of the evolution of χ_e^{HP} and χ_e drawn above is approximate. Such an interpretation implies that the values of χ_e^{HP} obtained earlier have to be reduced by 20-30% for most pulses and by a larger amount for hot ion H modes (about $0.7 m^2 s^{-1}$ with relaxation taken into account). This relaxation in χ_e^{HP} made the correlation between χ_e^{HP} and confinement in shots 26801 and 26792 even clearer. The ratio of χ_e^{HP}/χ_{eff} from Fig. 12, taking the relaxation of χ_e into account, varied between 0.8 and 2.

We have demonstrated that, based on the above interpretation of $\chi_e^{HP}(t)$, the $\tilde{T}(r,t)$ decay in the zone $r_{inv} < r < r_{mix1}$ can be studied with the new method.

4. RESULTS FOR LOW-q-DISCHARGES

The T_e (r, t) evolution during 8MW ICRH in a limiter 6MA pulse is shown in Fig. 13. The T_e(r, t) evolution on a faster time scale is shown in Fig. 14. It is clearly seen that the complete gradient zone lies between r_{inv} and r_{mix1}. The HPP was analysed for two very similar pulses, 18058 and 18074. The averaged χ_e^{HP} values obtained from 9 sawteeth in both pulses are shown in Fig. 15 by a solid line. A very strong dependence of χ_e^{HP} on r (χ_e^{HP} (r) ~ r^2) was obtained. The errors bars shown correspond to the variance in χ_e^{HP} obtained for each crash with the common radial dependence $\chi_e^{HP} \sim r^2$. The real errors may have been larger due to the strong radial dependence, especially for the region $r \sim r_3$. Let us also note that additional systematic errors could have arisen in the experimental data for $r > 0.75$ due to geometry and errors in $\nabla T_e/T_e$. The quality of the heat waves, as qualified by the parameter S, were also poor because of the very large values of r_{mix1} and $\nabla T_e/T_e$.

Other natural phenomena sometime give additional opportunities for HPP studies. One can see from Fig. 13 that an instability can occur at $r \leq r_{inv}$ which very quickly transports heat to the r_{22} region. Later, at $r \geq r_{23}$ this heat wave looks very similar to HPP. Such heat waves were studied on T-10 [15], and it was

shown that χ_{ein}^{HP} (let us name the χ_e^{HP} from an instability χ_{ein}^{HP}) can be significantly less then χ_e^{HP} from sawteeth. This type of HPP has not previously been studied on other devices.

The one-boundary method [4] has been applied to the JET pulse 18074 to obtain χ_{ein}^{HP}. One can see from Fig. 15 where the dashed curve shows χ_{ein}, that the χ_{ein}^{HP} values obtained are slightly less then χ_e^{HP} values. Therefore, at least in this regime, sawteeth induced HPP represents the electron heat transport but not other effects.

Let us make a brief comparison of results from the new method in the zone $r < r_{mix1}$ with previous results for $r > r_{mix}$. For the 5MA pulse 10925, P_{NBI} was varied from 7MW to 5MW. The average value $\chi_e^{HP} \sim 6.8 m^2 s^{-1}$ for $r = 0.8$ was obtained in [16]. In this study $\chi_e^{HP} \approx 3 m^2 s^{-1}$ at $r = 0.6$ when $P_{NBI} = 5MW$. For the 1.5MA pulse 25360, the value $\chi_e^{HP} \sim (6 \pm 2)\ m^2 s^{-1}$ for $r \sim 0.65$ was obtained with the "single boundary" method [4], and was in reasonable agreement (taking into account the radial dependence) with $\chi_e^{HP} \sim 4 m^2 s^{-1}$ for $r \sim 0.45$ obtained with the mixture method. It is often very difficult to determine where the boundary between short time scale enhanced transport effects and the traditional outward heat wave is located, especially for low-q pulses. Previous JET results [16] may have been partly affected by these processes, but not in a dramatic manner. The study of HPP at $r_{inv} \leq r \leq r_{mix1}$ using the "mixture" method, together with careful analysis of low amplitude outward HPP using previous methods enables a wide radial zone to be covered.

5. DISCUSSION AND CONCLUSIONS

A new method for studying sawteeth induced HPP has been described. The electron temperature perturbation profile in the region $r_{inv} \leq r \leq r_{mix1}$ was taken directly from ECE experimental data and was sufficiently accurate to allow us to separate in time the crash from the beginning of the $\tilde{T}_e$ (r, t) profile evolution used in the analysis of electron heat transport. The usual shift between the crash and the start of analysis was about 2 ms. The high amplitude of $\tilde{T}_e$ in the region $r_{inv} \leq r \leq r_{mix1}$ allowed us to analyse HPP from each sawteeth crash individually.

The method was applied to the analysis of HPP in 1.5MA - 6MA ICRH and NBI heated plasmas.

The decay of χ_e^{HP} in time following the sawteeth crash has been determined. A part of the observed decrease was connected with the decay of χ_e from an enhanced state created by the sawteeth crash and a part was connected with $\chi_e(T_e, \nabla T_e)$ dependence. The new method gives us the means to examine the relaxation of χ_e in time. For most pulses studied, this relaxation implied that the χ_e^{HP} values obtained, with the analysis starting 2ms after the beginning of crash, had to be reduced by 20-30%. The influence of the χ_e relaxation on χ_e^{HP} was stronger in hot ion H modes. We have demonstrated that the $\tilde{T}_e(r, t)$ decay in the zone $r_{inv} < r < r_{mix1}$ could be studied with the new technique. The heat wave, a few milliseconds after the sawteeth crash, behaved in an almost diffusive manner for most of the pulses examined. The picture of the evolution of χ_e presented above remains approximate and needs to be studied in more detail.

The analysis has demonstrated the complicated χ_e^{HP} dependence with plasma parameters. The analysis of HPP in 10MW on axis and mixed (on and off) ICRH in 3MA L mode plasmas together with the results of χ_{eff} variations in these pulses [12], support a model with strong χ_e^{PB} dependence upon ∇T_e rather than on T_e.

Some results for NBI heated 3MA pulses were also presented including examples of slow HPP found during hot ion H mode plasma. A correlation of slow HPP with regimes with very good confinement was clearly seen. The low values of χ_e^{HP} (about $0.7 m^2 s^{-1}$ with relaxation effects taken into account) in H modes with very good confinement represent good electron confinement and an absence of significant convective heat fluxes in these regimes (the upper limit of the convective velocity is about 0.4m/s).

The value χ_e^{HP} drops during the transition from a low power L mode to a very good confinement H mode, while the local T_e increases by a factor 4. No simple dependence $\chi_e^{PB}(T_e, \nabla T_e)$ can produce the χ_e^{HP} values obtained in all regimes L, H and VH.

The ratio χ_e^{HP}/χ_{eff} (with the relaxation of χ_e taken into account) varied between 0.8 and 2 for 1.5-5MA ICRH, NBI + ICRH heated plasmas with additional power ranging from 2 to 22MW and H, D, ^{4}He gas fill. We have found, in general, that

the variations of χ_e^{HP} due to parameter changes were consistent with those observed for χ_{eff}.

The χ_e^{HP} values obtained for 6MA ICRH heated limiter discharges have a strong radial dependence. The heat wave from an unidentified instability was also studied in these discharges. The corresponding values of χ_{ein}^{HP} were slightly less than χ_e^{HP}.

ACKNOWLEDGEMENTS

The authors wish to acknowledge J.G. Cordey, B. Balet, J. P. Christiansen, A.C.C. Sips and K. Thomsen for numerous fruitful discussions.

REFERENCES

[1] T-10 Group, in Controlled Fusion and Plasma Heating, (Proc. 12th Eur. Conf. Budapest, 1985), Vol 9F, Part II, European Physical Society (1985), 38.

[2] Neudatchin, S.V. Problems of Nuclear Science and Technology, Thermonuclear Fusion, issue 3 (1986), 47 (in Russian).

[3] Bagdasarov, A.A., Vasin, N.L., Esiptchyk, Yu.V., Neudatchin, S.V., Razumova, K.A., Savrukhin, P.V., Tarazyan, K.N., Sov. J. Plasma Phys. 13 (1987) 518.

[4] Neudatchin, S.V., Contr. Fus. and Plasma Heating, (Proc. 15th Eur. Conf. Dubrovnik, 1988), V12B, Part III, European Physical Society (1988), 1147.

[5] Callen, J.D., Jans, G.L., Phys. Rev. Lett., 38 (1977) 491.

[6] Tubbing, B., Lopes-Cardozo, N.J., Van der Wiel, M.L., Nucl. Fusion, 27 (1987), 1843.

[7] Riedel, K., Eberhagen, A., Gruber, O., et al., Nucl. Fusion, 28 (1988), 1509.

[8] Fredrickson, E.D., Callen, J.D., McGuire, K., et al., Nucl. Fusion, 26 (1986) 849.

[9] Lopes Cardozo, N.J., Sips, A.C.C., Plasma Phys. and Contr. Fusion, 33 (1991), 1337.

[10] Fredrickson, E.D., McGuire, K., Gavallo, A., et al., Phys. Rev., Lett., 65 (1990), 2869.

[11] Bagdasarov, A. A., Vasin N. L., Neudatchin S. V., Savrukhin P. V, in Plasma Physics and Controlled Nuclear Fusion Research, Proc. 15th Int. Conf, Washington, 1990), VI, IAEA Vienna (1991), 253.

[12] Cordey J. G. and the JET team in Plasma Physics and Controlled Fusion Research (Proc. 14th Int. Conf., Wurzburg, 1992), IAEA-CN-56/D-3-4.

[13] Balet, B., Cordey, J.G., Stubberfield, P.M., Plasma Phys. and Contr. Fus., 33 (1991), 1255.

[14] Cristiansen J. P., Balet, B. Boucher D., et al. Proceeding 19th European Conference on Controlled Fusion and Plasma Physics., Innsbruck 1992, Plasma Physics ans Controlled Fusion 34 (1992) 1881.

[15] Bagdasarov A.A., Neudatchin S.V., in Controlled Fusion and Plasma Physics, (Proc. 18th Eur. Conf. Berlin 1991), Vol 15C, Part II, European Physical Society (1991) 101.

[16] Lopez Cardozo N.J., de Haas J.C.M, Nucl. Fusion, 30, 1990, 521.

[17] Gondhalekar A., Cheetham, A.D., de Haas, J.C.M., et al. Plasma Phys. and Contr. Fusion 31 (1989) 805.

[18] Callen, J.D., Christiansen J.P., Cordey, J.G., et al., Nucl. Fusion 27 (1987) 1857.

[19] Rebut, P.H., Lallia, P.P., Watkins, M.L., in Plasma Physics and Controlled Nuclear Fusion Research 1988. (Proc. 12th Int. Conf. Nice, 1988), Vol. 2, IAEA, Vienna (1989), 191.

[20] Dnestrovskij Yu. N., Beresovskij, E.L., Lysenko, S.E., et al., Nuclear Fusion, 31 (1991), 1877.

[21] Balet, B., Boucher, D., Cordey, J.G., Muir, D.G., Neudatchin, S.V., Schmidt, G.L., in Controlled Fusion and Plasma Physics (Proc. 19th Eur. Conf. Innsbruck 1922), Vol 16 C, Part I, European Physical Society (1992) 59.

[22] Blum. J., Lazzarro, E., O' Rourke, J., et al., Nucl. Fusion 30 (1990) 1475.

[23] Dnestrovskii Yu. N., Neudatchin, S.V., Pereversev, G.V. Sov. J. Plasma Phys., 10, (1984), p137.

[24] Alikaev, V.V., Bagdasarov, A.A., Berezovskij, E.L., et al., in Plasma Physics and Controlled Nuclear Fusion Research 1986 (Proc. 11th Int. Conf., Kyoto 1986), Vol. 1, IAEA, Vienna (1987) 111.

[25] Costley, A.E., Baker, E.A.M., Bartlett, D.V. et al., in Electron Cyclotron Emission and Electron Cyclotron Resonance Heating (Proc. 5th Int. Workshop San Diego, CA, 1985) GA Technologies Inc., San Diego, CA (1985) 3.

[26] Muir D.G., JET Data Analysis and Modelling Unit Note DPA(93)02, JET Joint Undertaking, Abingdon, Oxon, OX14 3EA, 1993, "The Second Processing Chain."

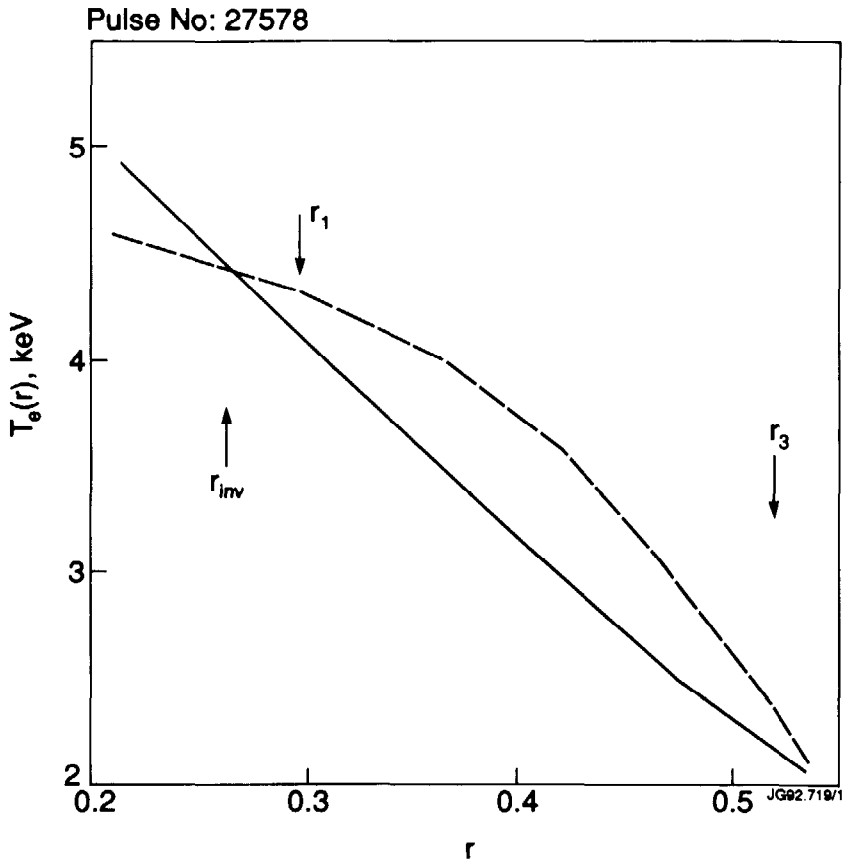

Fig. 1 The $T_e(r)$ profiles before and 1ms after beginning of a sawtooth crash for pulse 27578 (10MW on axis ICRH, 3MA).

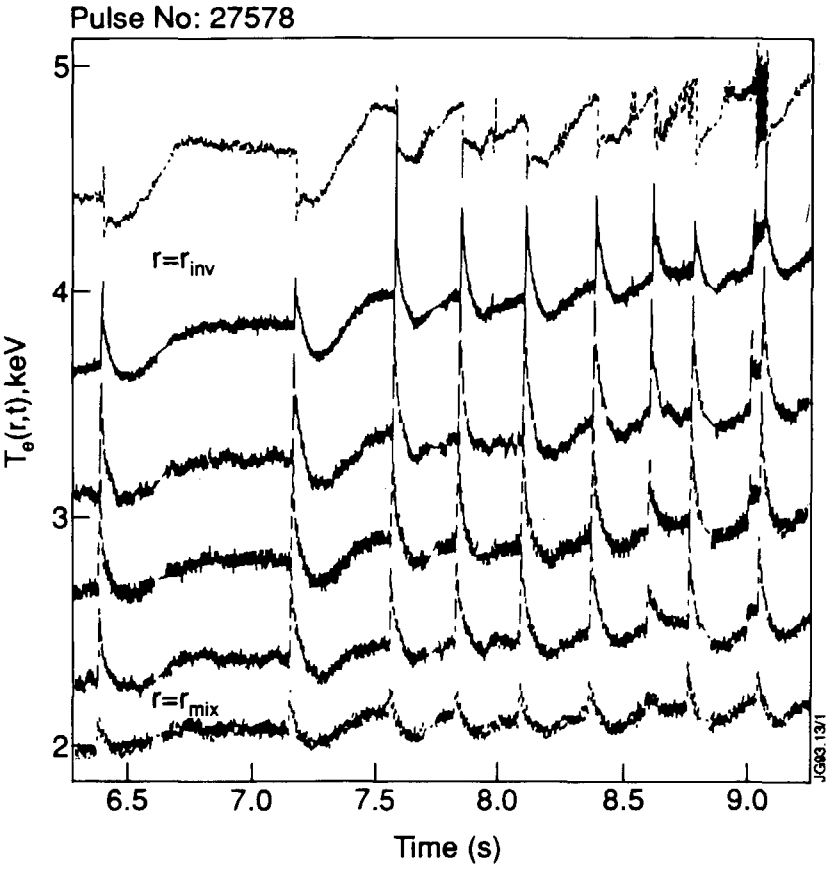

Fig. 2 $T_e(r,t)$ evolution for pulse 27578.

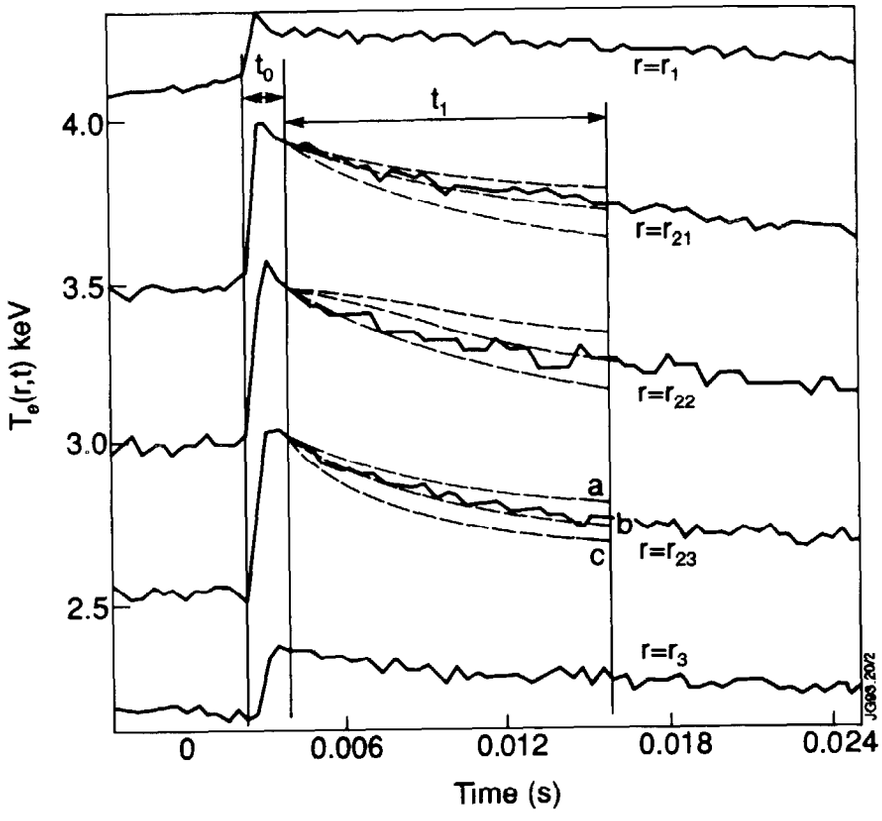

Fig. 3 An example of the evolution of $T_e(r, t)$ for pulse 27578, $\tilde{T}e\ (r_1, t)$ and $\tilde{T}e\ (r_{3,t})$ are the boundary conditions. The dotted curves a, b, c, are the results of calculations with $0.5\ \chi_{eo}^{HP}$, χ_{eo}^{HP} and $2.\chi_{eo}^{HP}$.

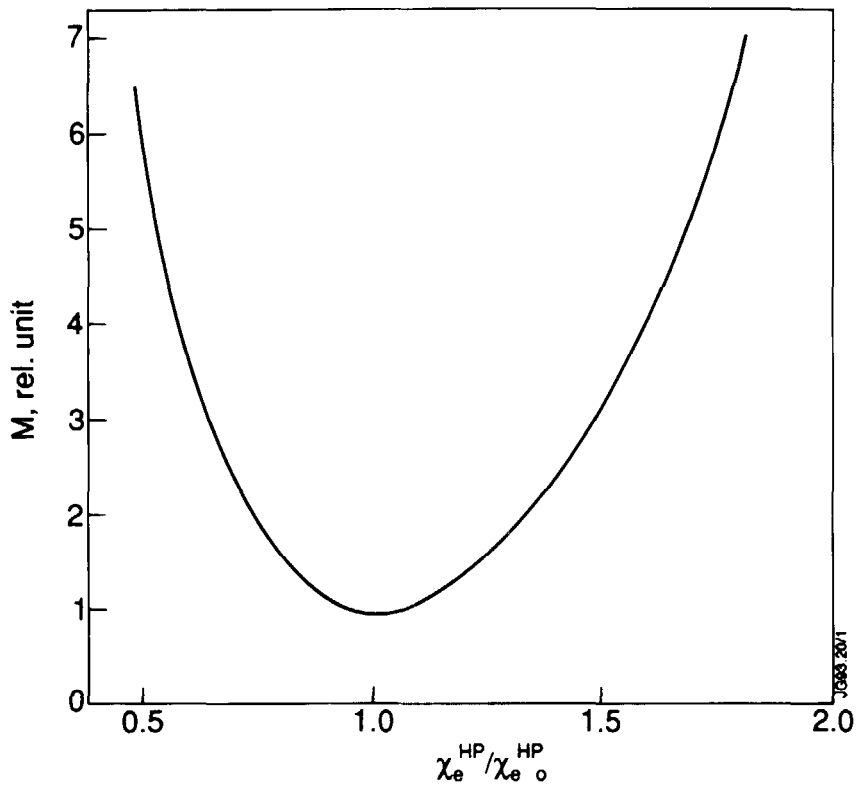

Fig. 4 The dependence of the sum of square differences between calculated and experimental data, M, to the normalised value of χ_e^{HP} for pulse 27578.

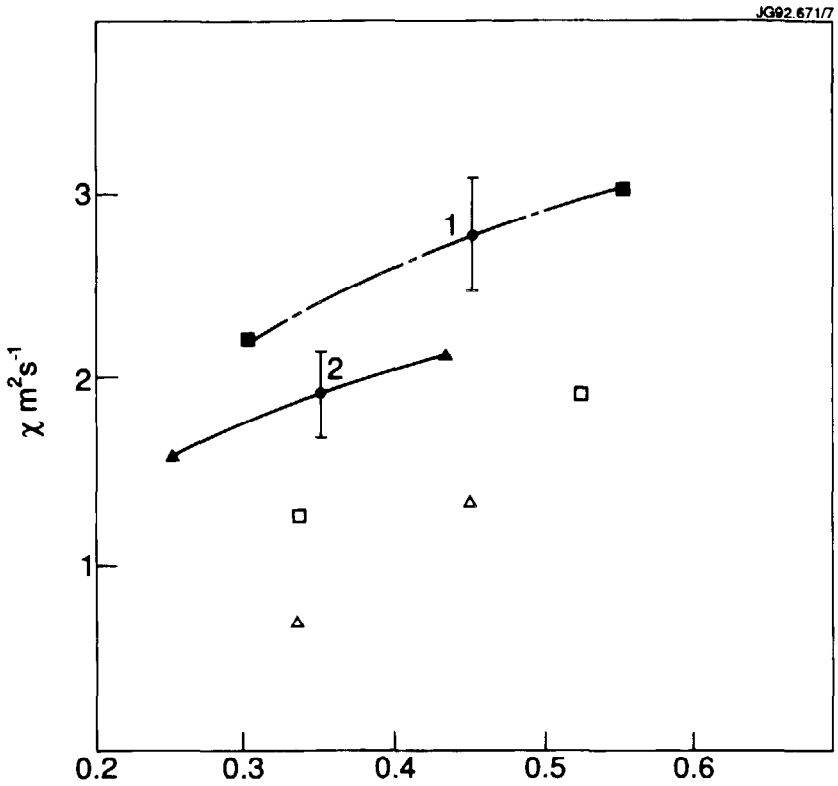

Fig. 5 The χ_e^{HP} (curves 1 and 2) and χ_{eff} values for 10 MW on-axis (#27578) and mixed (#27579) ICRH, I_p = 3 MA, S = 2.9 and 2.5.

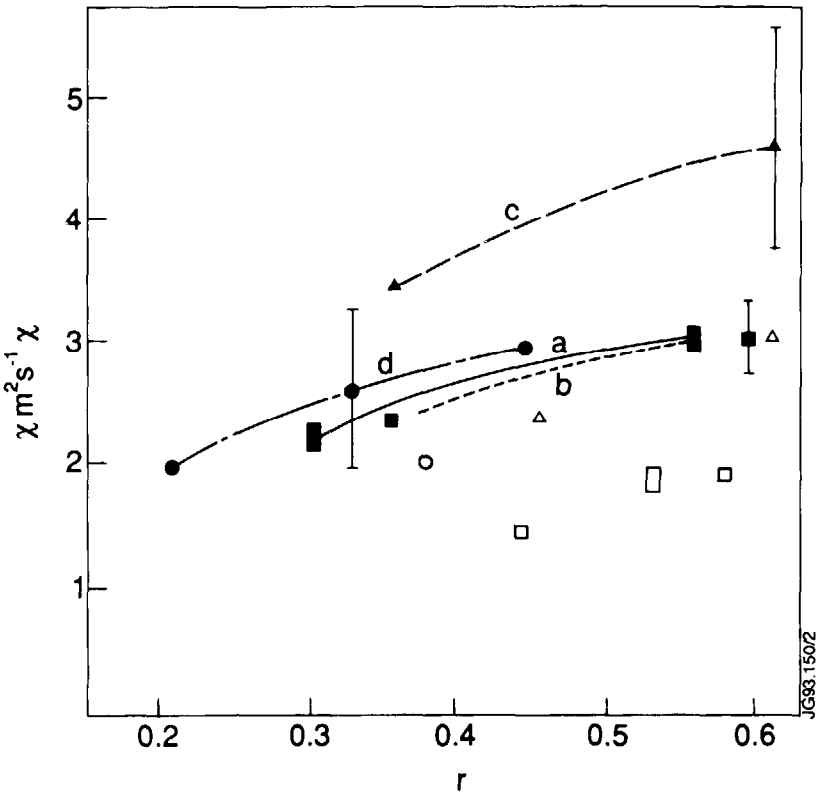

Fig. 6 The values of χ_e^{HP} and χ_{eff} for on axis ICRH with

a) 3 MA, 10 MW, #27578, S = 2.9, n_e (0.2) = 6.4 . 10^{13} m^{-3}
b) 3 MA, 8 MW, #25367, S = 1.2, n_e (0.2) = 5.5 . 10^{19} m^{-3}
c) 1.5 MA, 8 MW, #25360, S = 1.3, n_e (0.2) = 3.5 . 10^{19} m^{-3}
d) 1.5 MA, 4 MW, #25358, S = 2.4, n_e (0.2) = 3.0 . 10^{19} m^{-3}

T_e(0.4) relationship 1:1:0.8:0.5 for a:b:c:d

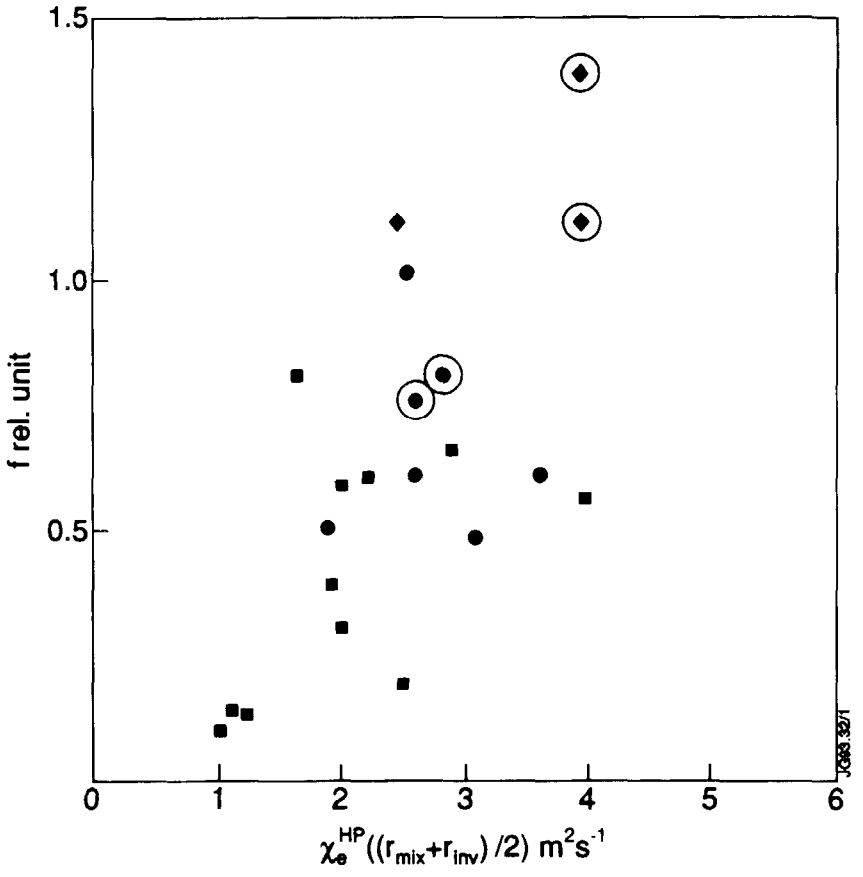

Fig. 7 The map of f values obtained for various pulses

◇ - 1.5 MA ICRH, • - 3 MA ICRH

□ - 3 MA NBI

$\chi_e^{HP} = f\,(r \cdot T_e(r)/r_{inv})^{3/2}\,r.$

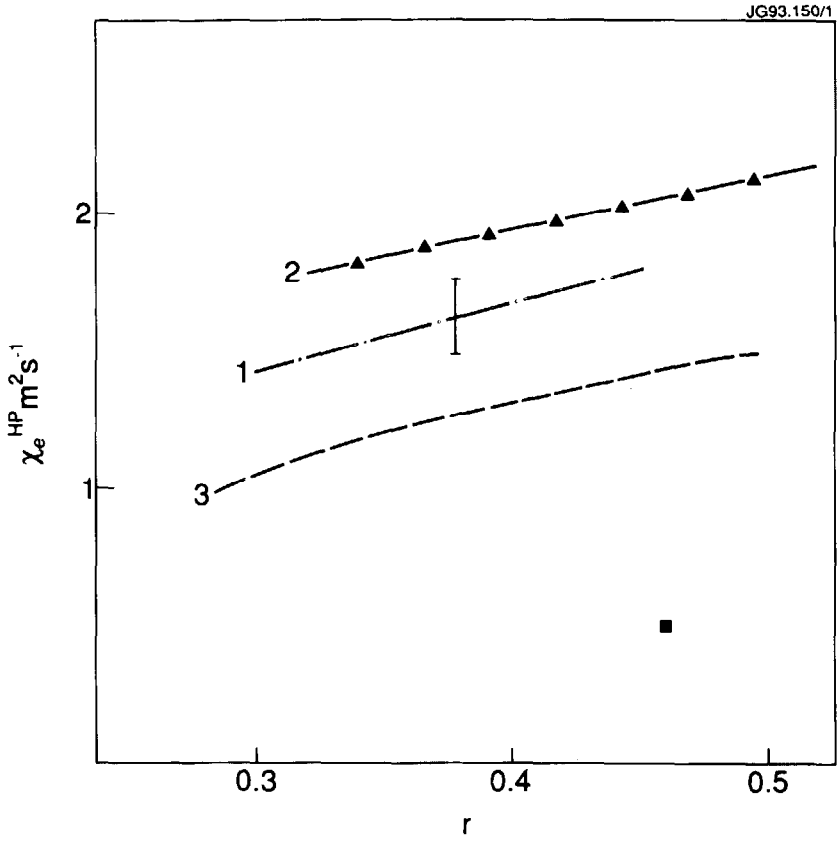

Fig. 8 χ_e^{HP} (curve 1) for 2 MW NBI and an over estimation of χ_e^{HP} (curve 2) at the end of an 11MW NBI hot ion H-mode. Identical pulses 26290 and 26292 were used. Error bars on curve 1 represents only the statistical variance of χ_e^{HP} values obtained for each crash separately, $n_e(0.4) \approx 2; 5; 4.10^{19}$ m^{-3} and S = 2; 4; 3.5 for curves 1, 2, 3; ■ and curve 3 - χ_{eff} and χ^{HP} for pulse 26801 (13MW hot ion H mode).

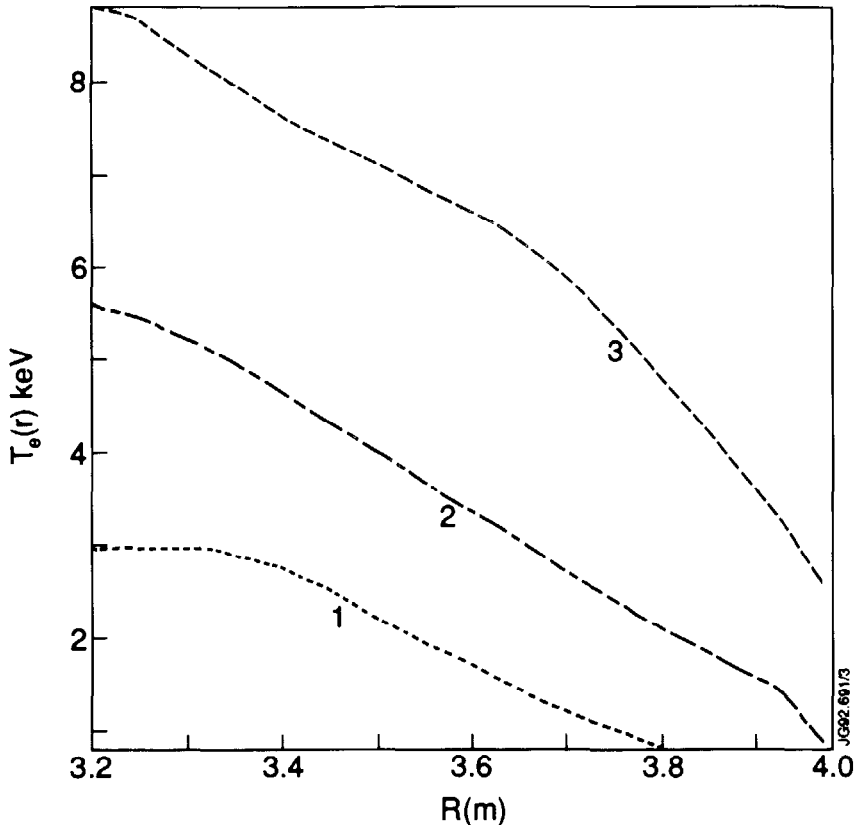

Fig. 9 Electron temperature profiles for curves 1, 2 and 3 from Fig. 8.

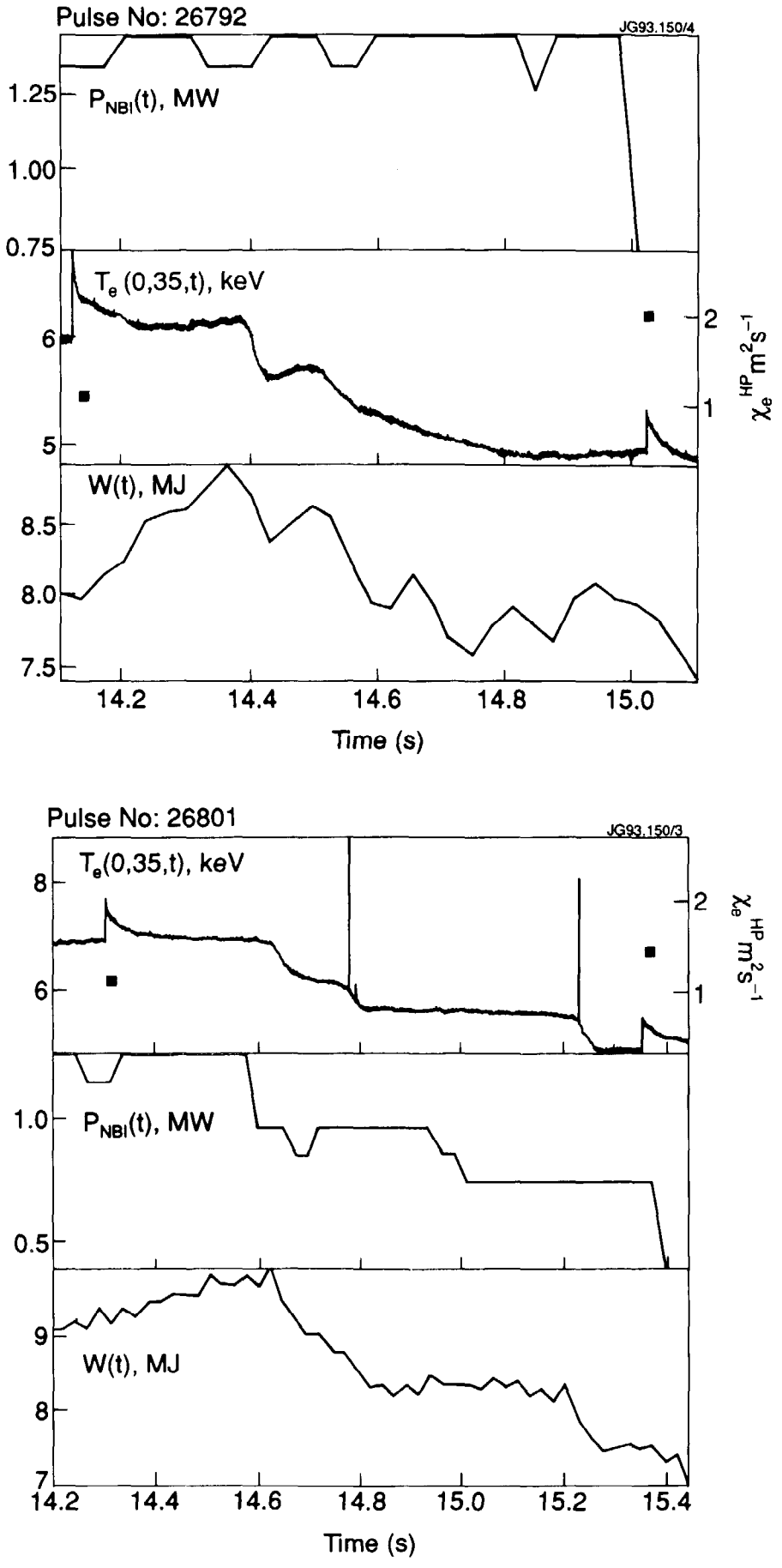

Fig. 10, 11 The evolution to $T_e(r, t)$ at $r \approx 0.35$, $P_{NBI}(t)$, stored energy W(t) and χ_e^{HP} in pulses 26792 and 26801.

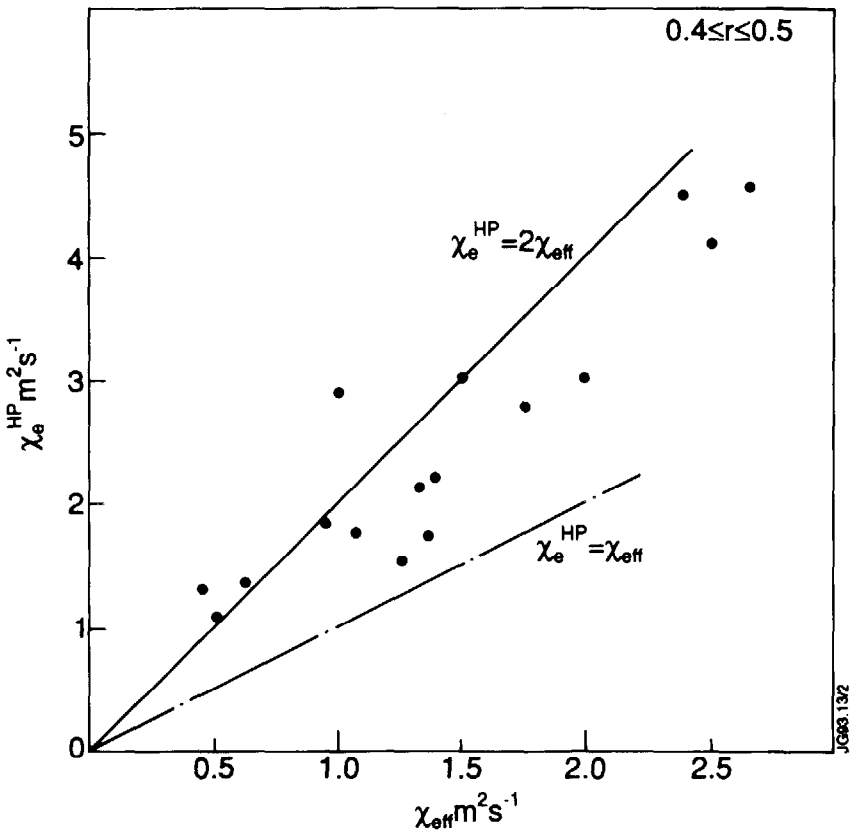

Fig. 12 Comparison of χ_e^{HP}, χ_{eff} for 1.5MA - 5MA plasmas, ICRH, NBI, ICRH + NBI, gas fill D, H, ^{4}He.

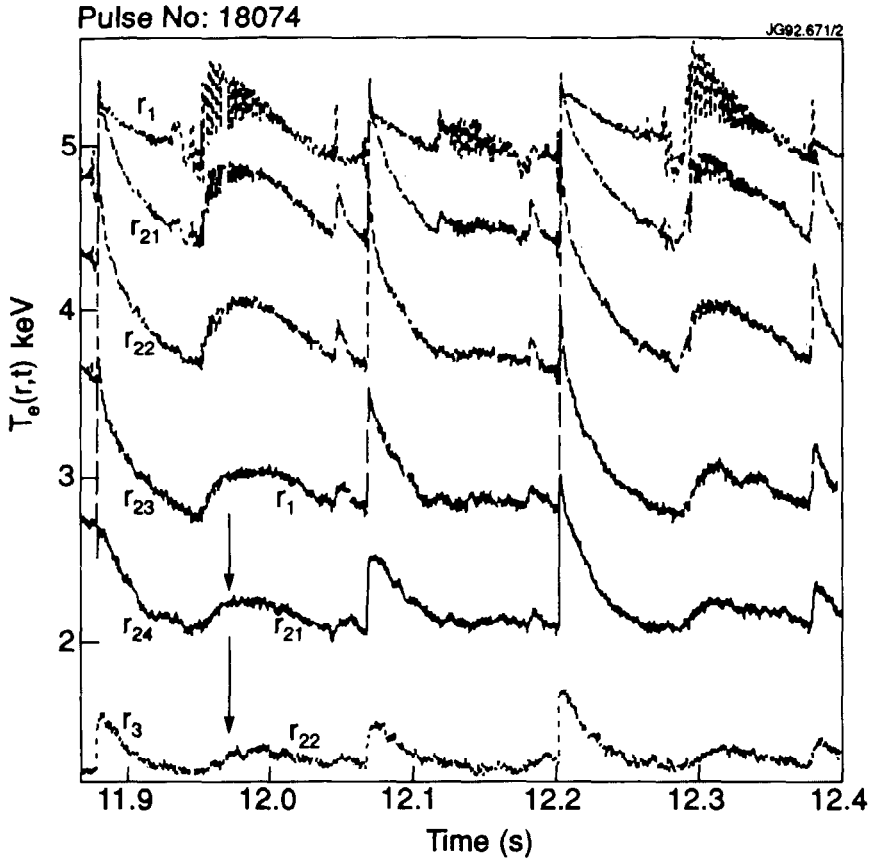

Fig. 13 T_e (r,t) evolution in 6 MA limiter discharge with 8 MW on axis ICRH (# 18074)

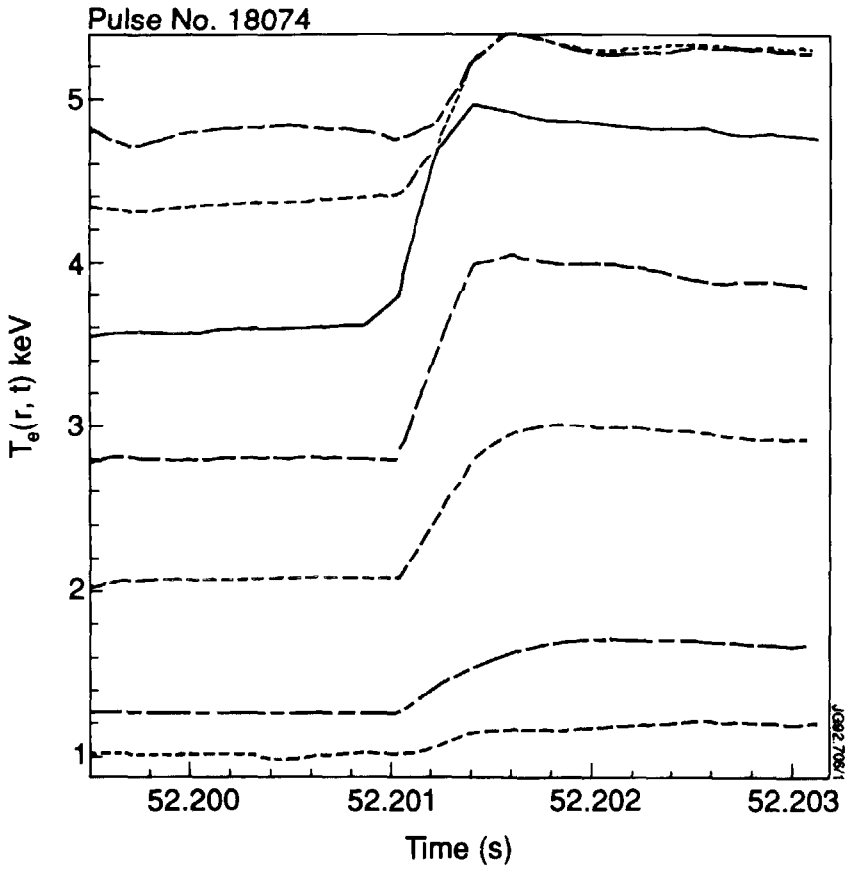

Fig. 14 Fast time scale $T_e(r,t)$ evolution for pulse 18074.

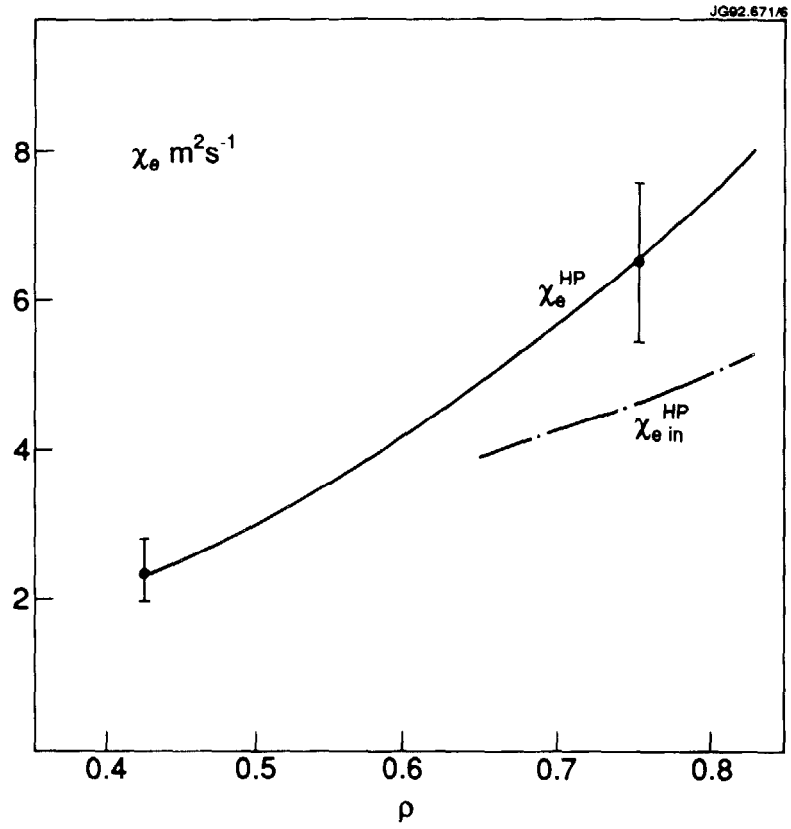

Fig. 15 χ_e^{HP} values for 6 MA pulses (#18074 and 18058), χ_{ein}^{HP} for pulse 18074. Error bars were determined from the variance of nine crashes in both pulses. S = 1.5 for sawteeth induced heat wave, and S = 2.2 for instability induced heat wave.